LED Nonlinearity Mitigation in a NOMA-OFDM VLC System Using a Union of Precoder and Companding

Nishant Sharan (nishant_er07@yahoo.com)
Birla Institute of Technology https://orcid.org/0000-0003-0075-9327
Swapan Kumar Ghorai
BIT Mesra: Birla Institute of Technology
Ajit Kumar
Rajiv Gandhi Memorial College of Engineering Technology

Research Article

Keywords: NOMA, DCO-OFDM, Precoder, Compander, PAPR, BER

Posted Date: March 3rd, 2022

DOI: https://doi.org/10.21203/rs.3.rs-1303622/v1

LED Nonlinearity Mitigation in a NOMA-OFDM VLC System Using a Union of Precoder and Companding

Nishant Sharan[1*], Swapan Kumar Ghorai[1] and Ajit Kumar[2]

[1*]Department of ECE, Birla Institute of Technology, Mesra, Ranchi, 835215, Jharkhand, India.

[2]Department of ECE, RGM CET, NH-40,Nerawada, Nandyal, Kurnool, 518501, Andhra Pradesh, India.

*Corresponding author(s). E-mail(s): nishant_er07@yahoo.com; Contributing authors: skghorai12@rediffmail.com; ajitk9kumar@rgmcet.edu.in;

Abstract

The power domain non-orthogonal multiple access (NOMA) has been considered as an outstanding candidate for 5G visible light communication networks. Due to the various salient features like robustness to multi-path fading, low latency, high compatibility with multiple input multiple output (MIMO) systems, etc. orthogonal frequency division multiplexing access (OFDM) is foreseen to exist in 5G systems. NOMA-based optical OFDM (O-OFDM) is expected to be a promising candidate for supporting high rate internet connectivity, especially for green indoor mobile networks. The OFDM waveform suffers from high PAPR issue. The high PAPR degrades the BER and also enhances the nonlinearity in an O-OFDM system. In this paper, a hybrid technique using a blend of precoder with compander is implemented to reduce the PAPR of NOMA based DC-biased O-OFDM (DCO-OFDM) system. The proposed NOMA DCO-OFDM system exhibits a low PAPR of only 4.3 dB. Also, for a reference bit error rate of 10^{-4}, the proposed technique displays an error vector magnitude (EVM) of 13.2 dB.

Keywords: NOMA, DCO-OFDM, Precoder, Compander, PAPR, BER

1 Introduction

An unprecedented proliferation in the usage of high-speed indoor data communication networks for different services like work from home (WFH), online education, internet of things (IoT), cloud storage etc., and the omnipresent internet connectivity in the past two years has resulted in a massive surge in the global data traffic. To deal with it, the current radio frequency (RF) bandwidth scheme has a significant problem coping with the required spectrum. The availability of vast unregulated visible spectrum demands a paradigm shift in the existing wireless system moving to mobile internet connectivity utilizing the lighting infrastructure. With the exception of serving illumination, visible light communication (VLC) makes use of LEDs' luminescence for high transmission capacity especially in indoor wireless networks [1]. Owing to the huge unlicensed spectrum, robust security, low cost, low latency, immunity to electromagnetic interference (EMI) etc., the VLC supports the green aspect of next-generation 5G/6G wireless networks with energy-efficient data transmission [1]. In an optical wireless system, the low 3-dB bandwidth ($\backsim$ 20 MHz) of LEDs used as the transmitter restricts to achieve the practicable system capacity. Due to its numerous advantages, orthogonal frequency division multiplexing (OFDM) modulation has been the state-of-the-art for improving system capacity during the last decade. OFDM is projected to play a crucial role in developing 5G communication networks owing to its scalability with multiple input multiple output (MIMO) technologies [2].

Non-orthogonal multiple access (NOMA) is a feasible approach for enhancing system capacity in the forthcoming fifth-generation (5G) VLC network due to its reduced latency and higher spectrum efficiency [3]. In contrast to orthogonal frequency division multiplexing access (OFDMA), users in NOMA have simultaneous access to both frequency and time, and are differentiated by their power domains [4]. NOMA in association with OFDM modulation format is anticipated to support low latency, improved spectral efficiency, and wider cell coverage [5]. To boost the capacity of the NOMA VLC system, several efforts have been undertaken to implement OFDM schemes [6, 7]. The DCO-OFDM method is used to improve the user holding range in a NOMA VLC system in [6] and [7].

During the inverse fast Fourier transform (IFFT), however, the accumulation of highly coherent data symbols frequently raises the peak magnitude of the output signal. To measure this phenomenon, the peak-to-average power ratio (PAPR) is used. A high PAPR OFDM signal is undesirable in an optical communication system due to the nonlinear voltage-current (V-I) relationship of LED employed as a transmitter. Nonlinear distortion and poor bit error rate (BER) are the major detrimental effects of a high PAPR system. In order to compensate for nonlinear distortion, the power amplifier's quiescent point in the linear zone must be backed off. It lowers the signal-to-noise ratio (SNR) at the receiver and reduces the efficiency of the amplifier. Nonetheless, using a power amplifier with a large dynamic range increases the overall system cost.

In recent times, several PAPR reduction methods have been investigated in 5G radio systems [5, 8–11]. However, to the best of knowledge, a few state-of-art exist for PAPR reduction in NOMA optical wireless systems [12, 13]. This paper proposes a hybrid approach based on the union of a precoder and a µ-compander to lower the PAPR and reduce nonlinear characteristics in NOMA-based OFDM-VLC systems for 5G applications. Previously, we used the orthogonal multiplexing access (OMA) scheme to successfully implement the approach for PAPR reduction and nonlinearity mitigation in DCO-OFDM and ADO-OFDM systems [14, 15]. The paper presents the extension of our work in [14]. The NOMA has been applied to multiplex two users with a single base station. The DCO-OFDM, a most commonly used method for obtaining non-negative signal in visible light communication has been used for uni-polar signal transmission [16].

2 Proposed NOMA DCO-OFDM Model

Multiplexing of two users on a single base station is considered in this study. Practically, two users are considered in the NOMA application to lower both the detection delay and computational complexity at the receiver [17]. Figure 1 depicts the implementation of the proposed NOMA O-OFDM system.

As illustrated in the figure, the modulated data of users 1 (U_1) and 2 (U_2) are individually pre-processed in the transmitter section of the proposed hybrid NOMA scheme using a precoding matrix (PM). The precoded information of both users is transmitted simultaneously using the superposition coding (SC) technique, and power allocation (PA) is performed based on the channel state information (CSI) of U_1 and U_2 [18]. The Hermitian symmetry (HS) operation is performed before the inverse fast Fourier transform (IFFT) to obtain a real valued time-domain signal. Direct current (DC) bias clipping is applied to the output of the IFFT to produce a non-negative real signal. The µ-law compander is applied to the time domain signal before it is passed through the OSRAM SFH 4230, a high power LED used for message broadcast.

The photodiode (PD) used as the receiver converts the optical signal to an electrical signal through the process of photodetection. The received electrical

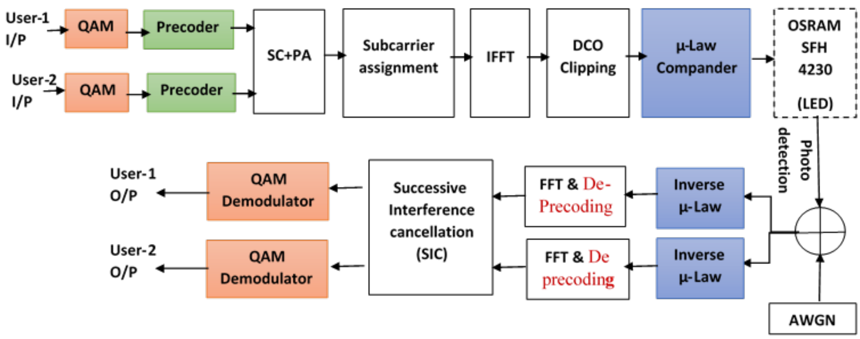

Fig. 1 Transceiver of the proposed NOMA DCO-OFDM system

signal is de-precoded after passing through the inverse μ-law compander. To separate the information of individual users, the principle of successive interference cancellation (SIC) is applied to the composite signal. Ultimately, the demodulator is used to recover the transmitted data from U_1 and U_2.

2.1 PAPR Computation

Let X_1 and X_2 represent the modulated symbols of user-1 (U_1) and user-2 (U_2) respectively. The modulated data are pre-processed in the frequency domain using a predetermined matrix P_M of the order R× Q given by [19]

$$P_M = \begin{bmatrix} p_{0,0} & \cdots & p_{0,N-1} \\ \vdots & \ddots & \vdots \\ p_{R-1,0} & \cdots & p_{R-1,Q-1} \end{bmatrix} \tag{1}$$

where R is $N+N_P$, Q is the number of base-band modulated data sub-carriers, N_P are nulls carriers used with $0 \leq N_P < N$. The precoded output signals are obtained as

$$Y_1 = P_M X_1 \tag{2}$$

$$Y_2 = P_M X_2 \tag{3}$$

The unit element of precoder matrix is defined as [19]

$$P_{m,k} = p_{m,0} e^{-j2\pi \frac{mk}{N}} \tag{4}$$

where $p_{m,0}$ is given by

$$p_{m,0} = \begin{cases} \frac{(-1)^m}{\sqrt{N}} \sin\left(\frac{\pi m}{2N_p}\right), & 0 \leq m < N_p \\ \frac{(-1)^m}{\sqrt{N}}, & N_p \leq m < N \\ \frac{(-1)^m}{\sqrt{N}} \cos\left(\frac{\pi(m-N)}{2N_p}\right), & N \leq m < R-1 \end{cases} \tag{5}$$

where $m \in \{0, 1, 2, ...R-1\}$ and $k \in \{0, 1, 2, ...N-1\}$. Assuming that channel state information of U_1 is superior to U_2, a fixed power NOMA approach is employed without loosing generality. The precoded NOMA signal $S[k]_{PNOMA}$ obtained as a result of superposition coding is expressed as [13]

$$S[k]_{PNOMA} = \sqrt{\alpha P_{tot}} Y_1 + \sqrt{(1-\alpha) P_{tot}} Y_2 \tag{6}$$

where α is the power allocation factor and P_{tot} is the total power of Y_1 and Y_2. The Hermitian symmetry (HS) yields an output vector that is double the length of original input sequence [14]

$$S[k] = \left[S_0 \cdots \; S_N \; \cdots S_{2N-K} \; \cdots \; S_{2N-1}\right]^T \tag{7}$$

and

$$S_{2N-K} = S_K^* \tag{8}$$

$S_{2N-K} = S_K^*$ is the complex conjugate of the vector $\mathrm{S_K}$. The result of the inverse fast Fourier transform (IFFT) followed by DC bias clipping produces a real-valued time-domain precoded NOMA-DCO signal, shown as [14]

$$Y(n) = \frac{1}{\sqrt{2N}} \left(2Re \sum_{i=0}^{N-1} S_i e^{\frac{j2\pi in}{N}} \right) \tag{9}$$

The time-domain precoded NOMA signal is subjected to the µ-law companding. As a result of the compander output, the recommended transmitted signal is given by

$$S(n)_{Proposed} = \frac{vlog\left(\frac{1+\mu|Y(n)|}{v}\right) sgn(Y(n))}{log(1+\mu)} \tag{10}$$

where μ denotes the compression control factor which extends from 0-255, v is the greatest amplitude and sgn indicates the signum function. The proposed transmitted time domain signal's PAPR is defined as the signal's maximum power divided by its mean power. Mathematically, it is computed as

$$\mathrm{PAPR(dB)} = 10\log_{10} \frac{|S(n)_{Proposed,max}|^2}{E|S(n)_{Proposed}|^2} \tag{11}$$

where $|S(n)_{Proposed,max}|^2$ denotes the maximum power and $\mathrm{E}|S(n)_{Proposed}|^2$ represents the mean power of the transmitted signal.

2.2 Proposed Receiver

At the receiver of the NOMA network, the base station (BS) receives the signal transmitted by each mobile user. With the assumption of reciprocal nature of the transmitter and receiver, the received signal is expressed as

$$R(n)_{Proposed} = \sum_{k=1}^{L} h_k \sqrt{\alpha P_{tot}} S_k(n) + n \tag{12}$$

L defines the overall number of users.
$\mathrm{h_k}$ relates to the $\mathrm{k^{th}}$ user's channel coefficient.
$\mathrm{P_{tot}}$ indicates total common usage power.
n is the normally distributed AWGN with 0 mean and standard deviation σ:

$$n \sim \mathcal{N}(0, \sigma^2)$$

As shown in Fig. 1, the inverse µ-law is applied to the received user signal followed by the FFT operation and de-precoding of the signal. The signal obtained as the result of the inverse µ-law operation is expressed as

$$R'(n) = \frac{v}{\mu} exp \left(\left| \frac{R(n)_{Proposed}(1+\mu)}{v} \right| - 1 \right) \tag{13}$$

3 Theoretical Evaluation of the Proposed NOMA DCO-OFDM System

The high PAPR in the NOMA DCO-OFDM system causes clipping distortion which degrades the net throughput of the system. In order to improve its transmission performance, the proposed scheme employs a precoder in conjunction with a µ-law compander. In precoding matrix (PM) approach, a predetermined matrix is used to pre-process the modulated data of each user in the frequency domain. In precoding matrix (PM) approach, the modulated data of each user is multiplied by a preset matrix P_M as indicated in Eqs. (2) and (3). The use of PM pre-processes data in the frequency domain by generating a cyclic shifted copy of the subcarrier waveforms. The variation in the shape of the subcarriers reduces the degree of auto-correlation among subarriers. So, this leads to the drop in the PAPR of the system due to the combination of low number of similar phase subcarriers. The application of µ-law compander to the precoded signal raises the average power of the signal. The increase in average power lowers the overall PAPR of the system.

The use of precoder decreases the clipping distortion which leads to improvement in the BER of the system. The uniform SNR distribution among data carriers degrades the BER. The SNR of i^{th} sub-carrier in a conventional OFDM is computed as [20]

$$\text{SNR(dB)} = 10\log_{10} \frac{|X(i)|^2}{\delta_i^2 + h_i^{-1}\psi_i^2} \tag{14}$$

where $|X(i)|^2$ is the power of i^{th} signal, δ_i^2 represents clipping distortion power, and $h_i^{-1}\psi_i^2$ is the channel noise power. The SNR of i^{th} precoded signal is given by

$$\text{SNR(dB)} = 10\log_{10} \frac{|X(i)|^2}{\frac{1}{N-1}\sum_{n=1}^{N-1}(\delta_i^2 + h_i^{-1}\psi_i^2)} \tag{15}$$

The use of precoder in presence of nulls modifies the $\frac{1}{N-1}\sum_{n=1}^{N-1}(\delta_i^2 + h_i^{-1}\psi_i^2)$ of the precoded NOMA DCO-OFDM signals. If $\frac{1}{N-1}\sum_{n=1}^{N-1}(\delta_i^2 + h_i^{-1}\psi_i^2) > \delta_i^2 + h_i^{-1}\psi_i^2$, the precoder lowers the SNR and BER of the system degrades. However, for i^{th} carrier if $\frac{1}{N-1}\sum_{n=1}^{N-1}(\delta_i^2 + h_i^{-1}\psi_i^2) < \delta_i^2 + h_i^{-1}\psi_i^2$, the precoder enhances the SNR to improve the BER of the system. So, the use of precoder with overhead (10% nulls) redistributes the SNR among different sub-carriers. As a consequence, each data carrier attains an average value. The overall improvement is obtained in presence of PM if the average SNR is sufficient for 16-QAM demodulator.

4 Results and Discussion

The performance of the proposed NOMA DCO-OFDM scheme is evaluated using the simulation results reported in this section. Complementary cumulative distribution function (CCDF), error vector magnitude (EVM) and BER are used to assess the performance of the proposed scheme. In this work, the modulated data is pre-processed using a predetermined matrix before IFFT. The output of IFFT is passed through a µ-law compander. The complete set of simulation parameters are presented in Table 1.

The CCDF is a statistical measure that is used to explain the probability distribution of the PAPR. Figure 2 depicts a CCDF comparison of NOMA DCO, precoded NOMA DCO, companded NOMA DCO, DCO-OFDM with precoder and compander, and the proposed NOMA system. The CCDF of the conventional NOMA DCO -OFDM is the same as obtained in [13]. The result depicts that the PAPR of the proposed hybrid NOMA DCO VLC system is

Table 1 Simulation Parameters (NOMA DCO-OFDM)

Data sub-carriers	64
IFFT lengths	32
Null carriers	3
DC Bias	5.1 dB
Cyclic prefix	25%

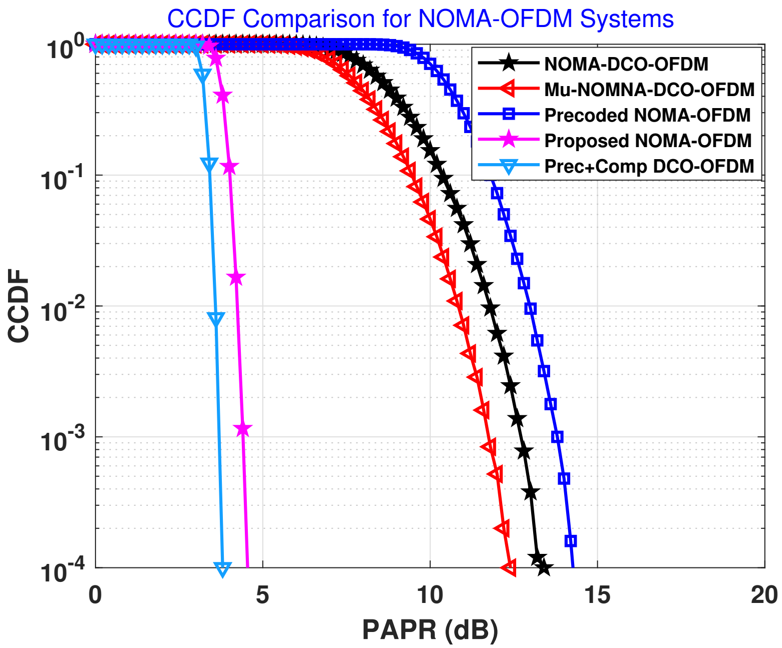

Fig. 2 PAPR comparison different NOMA DCO-OFDM systems

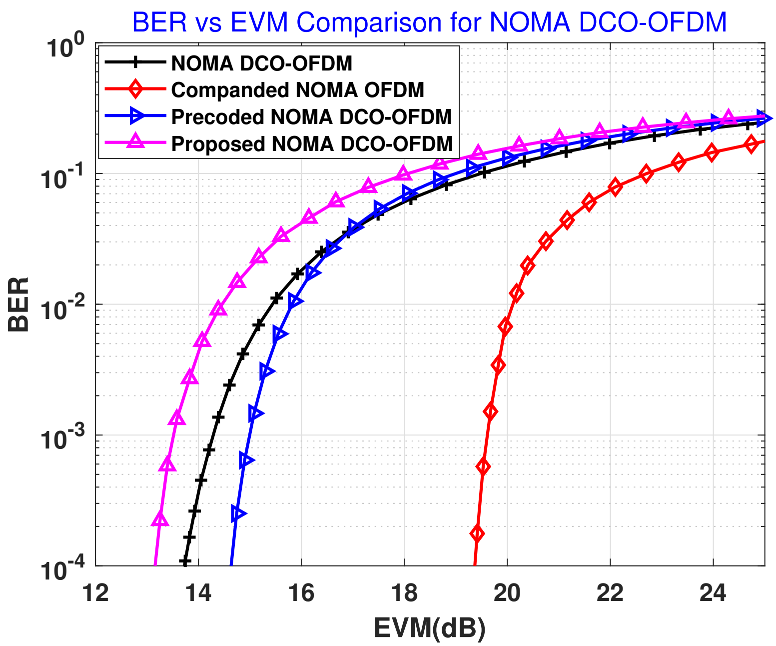

Fig. 3 BER comparison different NOMA DCO-OFDM systems

nearly 4.3 dB in comparison to 13.3 dB of the conventional NOMA. The pre-possessing of modulated symbols using a predetermined matrix followed by the µ-law algorithm increases the average power of the signal which results to low PAPR.

The root mean square (r.m.s) of the error vector is defined as the error vector magnitude (EVM), a metric that quantifies nonlinearity. The increased BER of the system is indicated by a high EVM. The BER comparison for different NOMA-OFDM Systems is shown in Fig. 3. The result illustrates that for a reference BER of 10^{-4} the nonlinearity of LED is least for the proposed system. As shown in Fig. 2, implementing the blend of precoder with compander to a conventional DCO-OFDM system gives low PAPR by a very small margin. However, the use of NOMA leads to enhance the capacity by supporting more users. Hence the proposed NOMA based O-OFDM system appears to be a good choice for high burst rate transmission to support the multi users.

Figure 4 shows a comparison of EVM performance for NOMA systems. The OSRAM SFH 4230 LED has been used for data transmission. The sixth order curve fitting approach, as outlined in previous works, matches the LED's V-I response curve [14, 15]. The EVM is computed in the presence of an LED for five different bias voltages in the range of 1.6 V -1.7 V. Figure 4 (a) depicts the EVM performance of various NOMA DCO schemes at 1.6 V with input backoff power ranging from 0 to 8 dB.

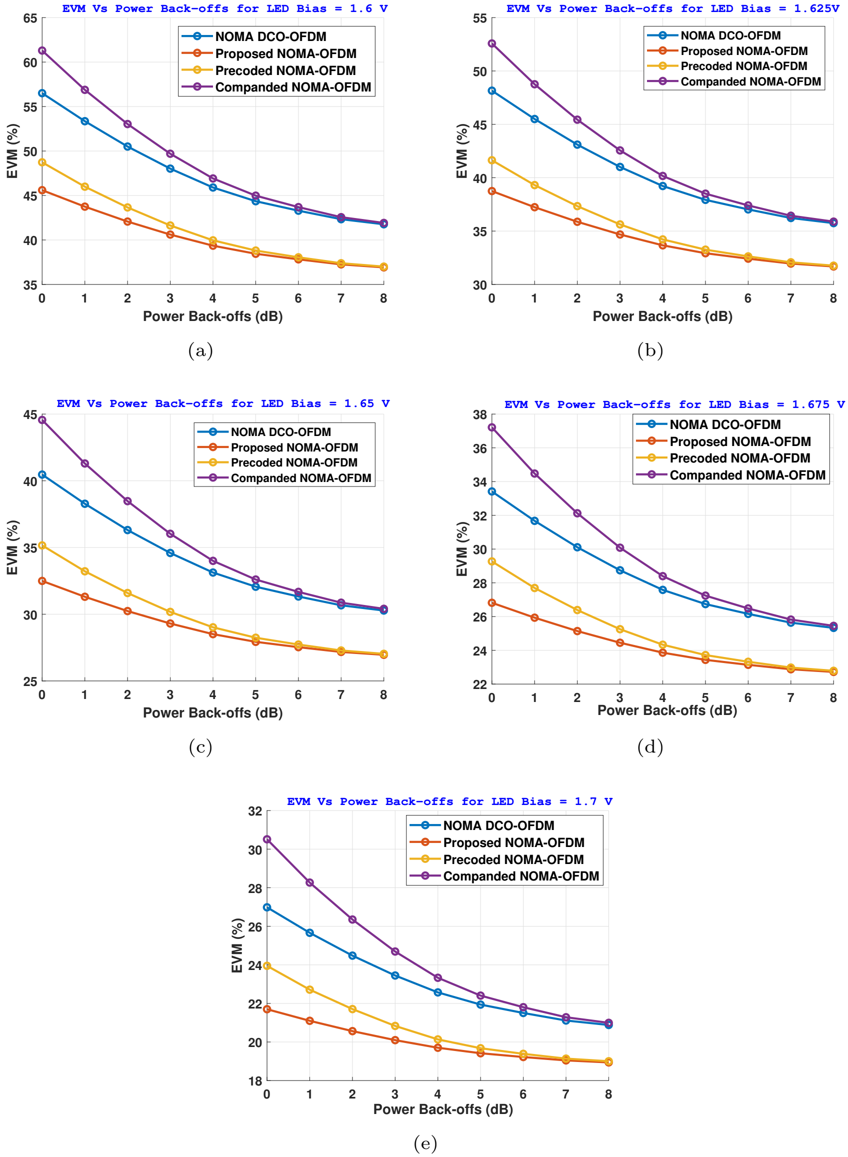

Fig. 4 Mean EVM comparison for different LED Bias Voltages (a) LED Bias=1.6 V, (b) LED Bias=1.625 V, (c) LED Bias=1.65 V, (d) LED Bias=1.675 V and (e) LED Bias=1.7 V

The information in Table 2 summarises the performance of each scheme. The μ-NOMA exhibits the highest EVM for all backoff values due to its nonlinear nature. The proposed scheme outperforms traditional NOMA, μ-NOMA, and Precoded NOMA in the range of 0-5 dB backoff power. However, at high

Table 2 EVM Comparison at LED Bias=1.6 V

	EVM (%)			
Backoff Power (dB)	µ-NOMA	NOMA	Precoded NOMA	Proposed NOMA
0	61.30	56.50	48.73	45.60
1	56.86	53.35	45.99	43.75
2	53.03	50.50	43.66	42.07
3	49.69	48.62	41.63	40.61
4	46.92	45.90	39.96	39.36
5	44.98	44.36	38.81.	38.45
6	43.69	43.29	38.65	38.05
7	42.56.	42.56	37.88	37.38
8	41.91	41.91	37.00	37.00

Table 3 EVM Comparison at LED Bias = 1.65 V

	EVM (%)			
Backoff Power (dB)	µ-NOMA	NOMA	Precoded NOMA	Proposed NOMA
0	44.56	40.47	35.16	32.49
1	41.30	30.28	33.22	31.31
2	38.48	36.31	31.55	32.24
3	36.03	34.59	30.17	29.30
4	34.00	33.12	29.02	28.51
5	32.60	32.06	28.24	27.93
6	31.67	31.33	27.73	27.73
7	30.86	30.76	27.28	27.28
8	30.40	30.40	27.30	27.30

backoff power levels of more than 6 dB, the precoded NOMA matches the performance of the proposed schemes.

Fig. 4 (c) depicts the performance of various schemes at 1.65 V and results are summarised in Table 3. As indicated in the table, the EVM of the suggested scheme drops to 32.49 % at 0 dB backoff, indicating a 13 % improvement over the same backoff at 1.6 V. In comparison to 1.6 V, the NOMA DCO scheme using the union of precoding and compander offers an improvement of more than 10% for higher backoff values of more than 5 dB.

Table 4 EVM Comparison at LED Bias = 1.7 V

	EVM (%)			
Backoff Power (dB)	µ-NOMA	NOMA	Precoded NOMA	Proposed NOMA
0	30.51	26.98	23.95	21.70
1	28.27	25.66	22.71	21.10
2	26.35	24.46	21.71	20.56
3	24.65	23.45	20.83	20.10
4	23.33	22.57	20.13	19.70
5	22.41	21.94	19.68	19.42
6	21.80	21.50	19.39	19.22
7	21.28	21.28	19.14	19.14
8	20.99	20.99	19.00	19.00

At 1.7 V, the combination of precoder and compander has the lowest EVM of 21.70 percent at 0 dB, as shown in Table 4, compared to 30.51 %and 26.98 % for µ-NOMA and traditional NOMA respectively.

In compared to conventional NOMA and Companded NOMA systems, the suggested system reduces nonlinearity for 0-5 dB input backoff power, resulting in higher power efficiency.

5 Conclusion

The power domain NOMA is one of the potential multiple access techniques for next-generation 5G wireless systems. In this paper, a hybrid approach using a conglomeration of precoder with compander is proposed for PAPR reduction and BER improvement in NOMA based DC-biased optical OFDM system. The proposed method supports the low PAPR and improved nonlinearity in a conventional NOMA DCO-OFDM system. The PAPR of the proposed hybrid NOMA DCO VLC system is approximately 4.3 dB, compared to 13.3 dB for the conventional NOMA. The application of NOMA in optical VLC systems manifests improved capacity regions in comparison to the OMA-VLC system. So, the improvement in nonliterary along with low PAPR makes the proposed system to be a good choice for the high-speed 5G indoor mobile data network.

Declarations

Funding

The work was supported by Birla Institute of Technology (BIT), Mesra under the Institute Research Fellowship (IRF) scheme - GO/Estb/Extn-Institute-F/Ph.D/2020-21/4231.

Conflict of interest

On behalf of all authors, the corresponding author states that there is no conflict of interest.

Availability of data and material

Not applicable

Authors’ contributions

All the authors have accepted responsibility for the entire content of this submitted manuscript and approved submission.

References

[1] Rehman, S.U., Ullah, S., Chong, P.H.J., Yongchareon, S., Komosny, D.: Visible light communication: A system perspective—overview and challenges. Sensors **19**(5) (2019). https://doi.org/10.3390/s19051153

[2] Sanchis-Borrás, C., Martínez-Inglés, M.-T., Molina-García-Pardo, J.-M., García, J.P., Rodríguez, J.-V.: Experimental Study of MIMO-OFDM Transmissions at 94 GHz in Indoor Environments. IEEE Access **5**, 7488–7494 (2017). https://doi.org/10.1109/ACCESS.2017.2691402

[3] Marshoud, H., Kapinas, V.M., Karagiannidis, G.K., Muhaidat, S.: Non-Orthogonal Multiple Access for Visible Light Communications. IEEE Photonics Technology Letters **28**(1), 51–54 (2016). https://doi.org/10.1109/LPT.2015.2479600

[4] Dai, L., Wang, B., Yuan, Y., Han, S., Chih-lin, I., Wang, Z.: Non-orthogonal multiple access for 5G: solutions, challenges, opportunities, and future research trends. IEEE Communications Magazine **53**(9), 74–81 (2015). https://doi.org/10.1109/MCOM.2015.7263349

[5] Baig, I.: A Precoding-Based Multicarrier Non-Orthogonal Multiple Access Scheme for 5G Cellular Networks. IEEE Access **5**, 19233–19238 (2017). https://doi.org/10.1109/ACCESS.2017.2752804

[6] Lin, B., Ye, W., Tang, X., Ghassemlooy, Z.: Experimental demonstration of bidirectional NOMA-OFDMA visible light communications. Opt. Express **25**(4), 4348–4355 (2017). https://doi.org/10.1364/OE.25.004348

[7] Valluri, S.P., Kishore, V., Vakamulla, V.M.: A New Selective Mapping Scheme for Visible Light Systems. IEEE Access **8**, 18087–18096 (2020). https://doi.org/10.1109/ACCESS.2020.2968344

[8] Huang, Y., Su, B.: Circularly Pulse-Shaped Precoding for OFDM: A New Waveform and Its Optimization Design for 5G New Radio. IEEE Access **6**, 44129–44146 (2018). https://doi.org/10.1109/ACCESS.2018.2864336

[9] Rateb, A.M., Labana, M.: An Optimal Low Complexity PAPR Reduction Technique for Next Generation OFDM Systems. IEEE Access **7**, 16406–16420 (2019)

[10] Fathy, S.A., Ibrahim, M., El-Agooz, S., El-Hennawy, H.: Low-Complexity SLM PAPR Reduction Approach for UFMC Systems. IEEE Access **8**, 68021–68029 (2020). https://doi.org/10.1109/ACCESS.2020.2982646

[11] Almutairi, A.F., Al-Gharabally, M., Krishna, A.: Performance Analysis of Hybrid Peak to Average Power Ratio Reduction Techniques in 5G UFMC

Systems. IEEE Access **7**, 80651–80660 (2019). https://doi.org/10.1109/ACCESS.2019.2916937

[12] Al-Gharabally, M., Almutairi, A.F., Krishna, A.: Performance Analysis of the Two-Piecewise Linear Companding Technique on Filtered-OFDM Systems. IEEE Access **9**, 48793–48802 (2021). https://doi.org/10.1109/ACCESS.2021.3068371

[13] Yang, Y., Chen, C., Zhang, W., Deng, X., Du, P., Yang, H., Zhong, W.-D., Chen, L.: Secure and private NOMA VLC using OFDM with two-level chaotic encryption. Opt. Express **26**(26), 34031–34042 (2018). https://doi.org/10.1364/OE.26.034031

[14] N.Sharan, Ghorai, S.K.: PAPR reduction and non-linearity alleviation using hybrid of precoding and companding in a visible light communication VLC system. Opt. Quant Electron **52**(304) (2020)

[15] Sharan, N., Ghorai, S.K.: Hybrid scheme of precoder with µ-law compander for PAPR reduction and nonlinearity improvement in ADO-OFDM system. International Journal of Communication Systems **34**(16), 4961 (2021). https://doi.org/10.1002/dac.4961

[16] Armstrong, J.: OFDM for Optical Communications. Journal of Lightwave Technology **27**(3), 189–204 (2009). https://doi.org/10.1109/JLT.2008.2010061

[17] Ding, Z., Fan, P., Poor, H.V.: Impact of User Pairing on 5G Nonorthogonal Multiple-Access Downlink Transmissions. IEEE Transactions on Vehicular Technology **65**(8), 6010–6023 (2016). https://doi.org/10.1109/TVT.2015.2480766

[18] Islam, S.M.R., Avazov, N., Dobre, O.A., Kwak, K.-s.: Power-Domain Non-Orthogonal Multiple Access (NOMA) in 5G Systems: Potentials and Challenges. IEEE Communications Surveys Tutorials **19**(2), 721–742 (2017). https://doi.org/10.1109/COMST.2016.2621116

[19] Slimane, S.B.: Reducing the Peak-to-Average Power Ratio of OFDM Signals Through Precoding. IEEE Transactions on Vehicular Technology **56**(2), 686–695 (2007). https://doi.org/10.1109/TVT.2007.891409

[20] Jiang, T., Tang, M., Lin, R., Feng, Z., Chen, X., Deng, L., Fu, S., Li, X., Liu, W., Liu, D.: Investigation of DC-Biased Optical OFDM With Precoding Matrix for Visible Light Communications: Theory, Simulations, and Experiments. IEEE Photonics Journal **10**(5), 1–16 (2018). https://doi.org/10.1109/JPHOT.2018.2866952